A Marie-Curie-ITN within H2020

migrate microfluidics

ISTEGIM 2019

Proceedings of the International Symposium on Thermal Effects in Gas flows In Microscale October 24-25, 2019 – Ettlingen, Germany

ISTEGIM 2019 - 285038

COMPARATIVE STUDY OF THE EVAPORATION COEFFICIENT PREDICTING METHODS USING MOLECULAR DYNAMICS SIMULATIONS

Moritz C.W. Wolf [*1,2], **Arjan J.H. Frijns**[2], **Silvia V. Nedea**[2], **and Ryan Enright**[1]

[1]**Nokia Bell Labs, Blanchardstown Business Technology Park Dublin, D15 Y6NT Ireland**
[2]**Eindhoven University of Technology, PO Box 513, 5600MB Eindhoven, the Netherlands**

KEYWORDS:

Molecular Dynamics, Evaporation/Condensation coefficient, Liquid-Vapor interphase, Kinetic boundary conditions (KBC), S-model kinetic equation

ABSTRACT

Kinetic theory and molecular dynamics play an important role in investigating non-equilibrium phenomenon at liquid-vapor interface where evaporation/condensation take place. A new alternative method to extract the evaporation/condensation coefficients on molecular level is presented as well as an overview of existing coefficient Molecular Dynamics (MD) extraction methods. The alternative method shows the advantage that no additional MD simulations are required to define the evaporation/condensation coefficient compared to the methods of Gu [1] and Ishiyama [2]. The influence of the liquid and vapor boundary position on the evaporation coefficient is investigated. Exploring different combinations of the methods, provides multiple coefficients for each temperature T between the boiling ($T_b = 87.3K$) and critical ($T_C = 150.7K$) temperature of Argon. For an equilibrium liquid-vapor system of Argon, the results include an average evaporation coefficient $0.9 \geq \overline{\alpha_e} \geq 0.4$ as function of temperature with standard deviation $0.07 \geq \sigma \geq 0.04$. Comparison between our results and literature data shows that most data falls within the confidence bounds and confirms that, at equilibrium, the coefficients decrease with increasing temperature. Using the half-range Maxwellian assumption for the distribution of the outgoing mass fluxes from the liquid to vapour phase results in higher evaporation coefficients when compared to corresponding values based on molecular computed fluxes. Depending on the vapour boundary position, this results in often unrealistic ($\sigma_e > 1$) evaporation coefficients at low temperatures.

1. Introduction

Evaporation and condensation is a non-equilibrium process which has many applications in different fields including biology, astronomy, physics, chemistry and engineering [3]. Accurate models to describe the transfer of mass and energy across the liquid-vapor interface have become increasingly important in recent years [4] and are seen as a key to design and development of future high-performance

[*] *corresponding author:* moritz.wolf@nokia.com

two-phase microscale cooling systems [5]. In principle, molecular dynamics (MD) can describe this process precisely. However, due to the large computational cost of MD, practical modelling typically consists of a multiscale approach in which continuum, e.g. Navier-Stokes and gas kinetics, e.g. BGK, S-model [6], DSMC models are used to capture heat/mass transfer in the bulk. MD can be used to study the liquid-vapor interface on the molecular scale to generate the appropriate molecular parameters to the kinetic boundary condition (KBC). In particular, accurate definition of coefficients appearing in the KBC as a function of system operating conditions are of particular interest in order to refine predictive models. Here we highlight different techniques that have been demonstrated in the literature to define these coefficients from MD simulation results and present our own analysis which includes the results of our new alternative method. The results of our analysis are used to define rational confidence bounds on the evaporation and condensation coefficient for Argon in equilibrium for temperatures between the boiling ($T_b = 87.3K$) and critical ($T_C = 150.7K$) temperature. In the next section, the definition of the evaporation/condensation coefficient is given in terms of mass fluxes. The evaporation extraction methods of Meland [7], Gu [1] and Ishiyama [2] are briefly explained and our alternative method is introduced and in detail presented. Thereafter, the properties of the equilibrium molecular dynamics simulations are given. In section results, we show the average evaporation coefficient $\overline{\alpha_e}$ and its $\pm 1\sigma$ confidence bounds as function of temperature. These results are compared with the coefficients obtained using the half-range Maxwellian distribution for the outgoing mass flux. The final section contains our conclusions of the present study.

2. Liquid-Vapor boundary

The kinetic theory is capable of describing the vapor flow in combination with suitable KBC to describe the liquid-vapor interface. As mentioned, they play an important role, because they describe the interaction of the vapor with its condensed phase in the interphase region. In kinetic theory, it is assumed that the interphase region (Knudsen layer) has zero thickness [7].

The fraction of molecules which condense to the total colliding molecules on the condensed phase is termed the condensation coefficient (α_c). The fraction of evaporated molecules to the total outgoing molecules from the condensed phase is defined as the evaporation coefficient (α_e). The part $(1-\alpha_c)$ vs $(1-\alpha_e)$ are those molecules which reflect back into the vapor vs condensed phase respectively.

At the molecular level, these coefficients are defined as,

$$\alpha_e = \frac{\langle J_{evap}\rangle}{\langle J_{evap}\rangle + \langle J_{ref}\rangle} = \frac{\langle J_{evap}\rangle}{\langle J_{out}\rangle}, \qquad \alpha_c = \frac{\langle J_{cond}\rangle}{\langle J_{cond}\rangle + \langle J_{ref}\rangle} = \frac{\langle J_{cond}\rangle}{\langle J_{coll}\rangle} \tag{1}$$

where $\langle J_{...}\rangle$ is the time-averaged mass fluxes of the evaporating, condensing, outgoing, colliding and reflecting molecules. To properly account for these fluxes in MD simulations, it becomes necessary to define liquid and vapor boundaries in the interphase region, see Fig.1.

In the case of an equilibrium state ($\alpha_e = \alpha_c$), it is assumed that the molecules colliding with the liquid-vapor interface will reflect diffusively and that distribution function of the colliding molecules is given by the half-range Maxwellian $f_e(\boldsymbol{\xi})$ with $\boldsymbol{\xi}\cdot\boldsymbol{n} < 0$. Hence, the mass flux from the liquid to the vapor phase is defined as [2],

$$\langle J_{out} \rangle_e = \int_{\xi_z>0} \xi_z f(\overline{\boldsymbol{x}}, \boldsymbol{\xi}) d\boldsymbol{\xi} = \int_{\xi_z>0} \xi_z f_e(\boldsymbol{\xi}) d\boldsymbol{\xi} = \rho_v \sqrt{\frac{RT_L}{2\pi}} \tag{2}$$

where we have assumed a planar interface such that $\boldsymbol{\xi} \cdot \boldsymbol{n} = \xi_z$ the velocity component perpendicular to the interface. Eq. (2) is the outgoing mass flux at the equilibrium state.

In Fig.1, the liquid boundary can be considered as the "end" of the liquid phase and the vapor boundary as the "beginning" of the vapor phase. In between an interphase layer is defined.

In our previous study [8, 9] we observed a large discrepancy in the heat flux and energy flux between the numerical results of the MD simulations and the steady-state S-model equation. This was traced back to the precise definition of the liquid and vapor boundary positions in the MD simulations used to extract coefficients for the KBC. The implication of this boundary position in different methods used to derive the evaporation/condensation coefficients is investigated.

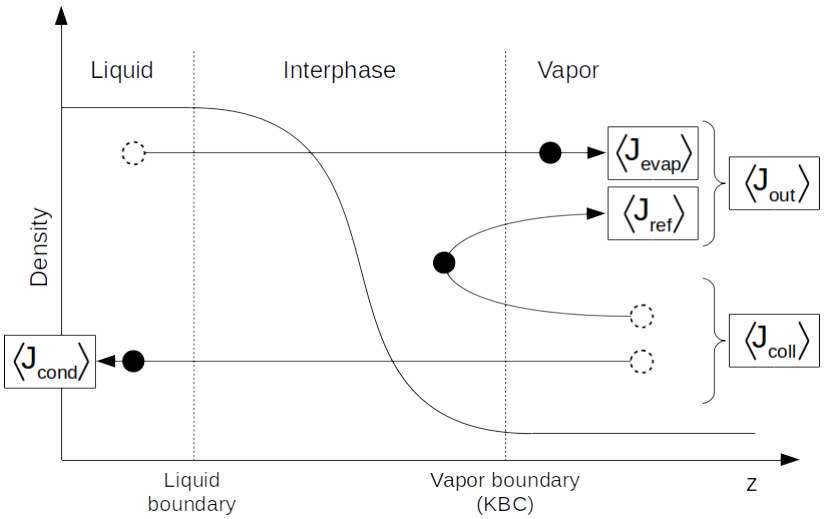

Figure 1: Schematic of the liquid-vapor interphase and the corresponding mass fluxes [10]

Meland et al. [7] used a geometrical definition to locate the liquid boundary. It is defined as the position where a tangent line attached at $(n_\infty + n_{liq}^{max})/2$ in the density profile crosses the line given by n_{liq}^{max}. Here, n_∞ is the vapor density far away from the interphase and n_{liq}^{max} is the maximum density attained in the liquid phase. The vapor boundary position is defined using the Soave-Redlich-Kwong (SRK) equation of state. It is the position near the interphase where pressure difference $|p_{MD} - p_{SRK}|$ becomes greater than the $max(|p_{MD} - p_{SRK}|)$ in the vapor phase, i.e. larger than statistical fluctuations. Hence, both definitions are based on macroscopic properties. Gu et al. [1] mentioned that this way of defining both boundaries is impractical for an unsteady non-equilibrium state where a liquid layer keeps growing or decreasing due to the evaporation and condensation. The statistical noise of the MD results will make it difficult to use both methods to locate the liquid and vapor boundary without having enough quasi-steady samples.

Gu et al. [1] focussed on a new procedure to address the problems of Meland [7]. They used a microscopic approach in which the location of the liquid and vapor boundary are based on the average number of interaction partners $\overline{N_k'(t)}$ per molecule per bin k. To determine the position of

the boundaries, two criteria values, C_v and C_l are set as the limit on $\overline{N'_k(t)}$ to consider the fluid to be in the vapor or liquid phase. When moving from the liquid to the vapor phase, the first bin for which $\overline{N'_k(t)} < C_l$ is recorded as the bin in which the liquid boundary is located. Similarly, the vapor boundary is locate in the first bin for which $\overline{N'_k(t)} > C_v$ when moving from the vapor to the liquid phase. The precise location of the liquid/vapor boundary within the bin is determined by the position of the molecule which has the largest/smallest number of interaction partners respectively. The limit values, C_l, C_v, are obtained from separate MD simulations of pure liquid and pure vapor. Hence, for an equilibrium simulation at temperature T it requires two additional MD simulations. Whereas for a non-equilibrium simulation with temperature T_1 and T_2, 4 additional MD simulations are needed. Furthermore, in case of non-equilibrium it becomes unclear at which temperature the additional MD simulations should be performed. Due to evaporation and condensation, a temperature gradient exists in the liquid and vapor phase.

Ishiyama et al. [2] calculated the evaporation coefficients in equilibrium state by introducing the concept of the spontaneously evaporating mass flux $\langle J^{sp}_{evap}\rangle$. The coefficient, according to [2], is defined as,

$$\alpha_e = \frac{\langle J^{sp}_{evap}\rangle}{\langle J_{out}\rangle_e} = \alpha_c \tag{3}$$

where $\langle J_{out}\rangle_e$ is defined in Eq. (2). The spontaneously evaporating mass flux is obtained from simulations of evaporation into vacuum. A vacuum boundary is placed within the vapor phase close to the interphase. Molecules that cross this boundary will be removed, hence no molecules can come back from the vacuum side. The vacuum boundary is located far enough from the liquid-vapor interphase such that at positions $z^* < z_{vacuum-boundary}$ the net mass flux of molecules is equal to the outgoing mass flux of molecules i.e. $(\langle J_+\rangle - \langle J_-\rangle)|_{z^*} = \langle J_+\rangle|_{z^*}$. The net mass flux of molecules is defined as $\langle J_+\rangle - \langle J_-\rangle$ with $\langle J_+\rangle$ the outgoing mass flux and, $\langle J_-\rangle$ is the colliding mass flux. The spontaneously evaporating mass flux is defined as [2],

$$\langle J^{sp}_{evap}\rangle = \langle J_+\rangle - \langle J_-\rangle = \langle J_+\rangle|_{vacuum-boundary} \tag{4}$$

Using this method, defining the liquid and vapor boundary location becomes redundant. However, Kobayashi [10] used this concept to improve the previous methods [1, 7] of determining the liquid and vapor boundary positions. An average position $\overline{z}$ can be calculated from the positions $z^* < z_{vacuum-boundary}$ at which the net mass flux is equal to outgoing mass flux. The vapor boundary position was defined at the average position $\overline{z}$. The liquid boundary location was set at the position where the spontaneously evaporating mass flux $\langle J^{sp}_{evap}\rangle$ from the vacuum simulations is equal to the evaporating mass flux $\langle J_{evap}\rangle$ from equilibrium simulations. According to [10], this method is appropriate to determine the liquid and vapor boundary in equilibrium and non-equilibrium simulations as well as multi-component systems. Similar to the previous method, additional MD simulations (into vacuum) have to be performed to calculate the mass flux.

We developed an **alternative method (Wolf)** which rely on shifting the vapor boundary position. This method explores the behaviour of the evaporation coefficient (Eq. (1)) in the interphase region. Applying one of the existing methods [1, 2, 7] to define the liquid boundary, the vapor boundary is shifted from the liquid to the vapor phase and thereby extracting the coefficient. Fig. 2 depicts the behaviour for different liquid boundary positions Z_{L_b} (randomly chosen). The alternative method defines

the maximum value attained in the interphase/vapor region as the evaporation coefficient, denoted by the black dot in the figure. The position of this maxima could be regarded as the location of the vapor boundary. Hence, no additional simulations are needed to define the vapor boundary position or evaporation coefficient. Depending on which method is used for the liquid boundary, additional simulations may be required.

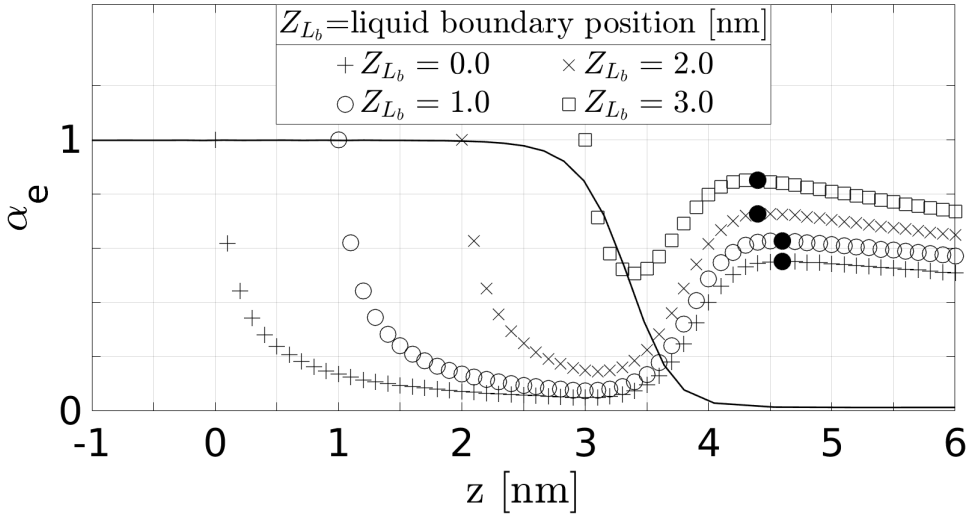

Figure 2: The behavior of the evaporation coefficient α_e for different liquid boundary positions $Z_{L_b} = 0.0 - 3.0nm$. The results corresponds to an equilibrium MD simulation in which $\alpha_e = \alpha_c$. The solid line represents the normalized density profile $\rho^* = \rho/\rho_L$. Black dots defines the evaporation coefficient for different liquid boundary positions (randomly chosen) according to the alternative method.

3. Equilibrium Molecular Dynamics simulation

The system to extract the evaporation and condensation coefficients consists of Argon vapor confined between its condensed phase as show in Fig. 3. Software package LAMMPS[11] has been used to execute the equilibrium MD simulations. The system contains between $N = 8000 - 10000$ molecules depending on the temperature which ranges from $T = 90{-}150K$ $(T/T_C = 0.6{-}1)$. This corresponds to a liquid-vapor equilibrium above its boiling point $T_b = 87.3K$ and below its critical point $T_C = 150.7K$. A Nosé-Hoover thermostat is applied within the grey regions denoted by T in Fig. 3 to control the temperature. The dimensions of the simulation domain are $L_x = L_y = 5.7nm$ and $L_z = 75.0nm$. The intermolecular forces between the Argon atoms are calculated using the 12-6 Lennard-Jones potential,

$$U(r) = 4\epsilon\left[\left(\frac{\sigma_D}{r}\right)^{12} - \left(\frac{\sigma_D}{r}\right)^{6}\right] \tag{5}$$

where the molecule diameter $\sigma_D = 0.3405nm$ and energy $\epsilon/k_b = 119.8K$ (k_b is the Boltzmann constant). The cut-off distance is set to $1.5nm$[2]. Periodic boundary conditions are imposed in all three directions. To obtain steady-state, the center of mass position of the system has been fixed to avoid drifting of the atoms in any direction during the simulation. Newton's equation of motion are solved with time step of 4fs. After steady-state is obtained, the simulation continued for 20000000 time step ($80ns$) and the configuration of the molecules has been extracted every 500 steps. Hence, $N_s = 2 \times 40000 = 80000$ data sets (two liquid-vapor interfaces) are used to extract the evaporation/condensation coefficient. The macroscopic properties are obtained by dividing the z-direction of

the simulation domain into bins and time-averaging over the extracted data. The liquid and vapor properties (pressure, density, temperature) are within 5% of the NIST-REFPROP [12].

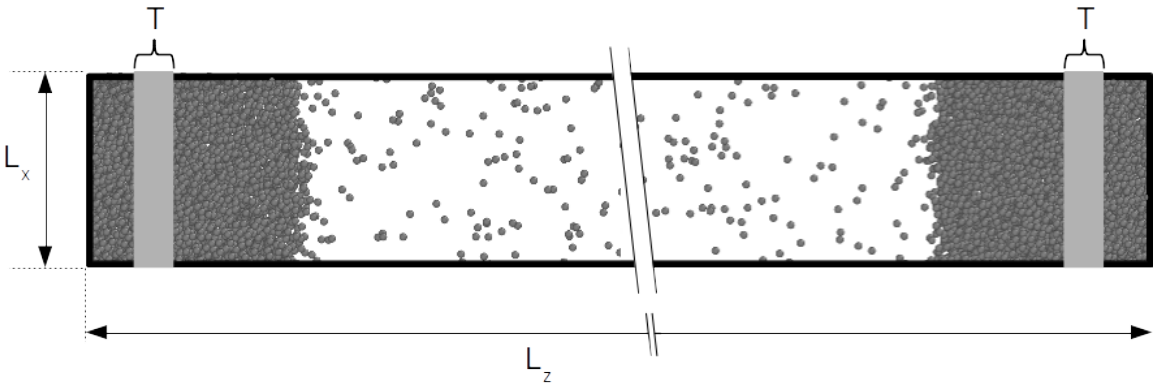

Figure 3: Schematic of the MD simulation domain. Grey area denotes the region of the Nosé-Hoover thermostat.

4. Results

As shown in Fig. 2, the position of the liquid boundary Z_{L_b} influence the behaviour of the evaporation coefficient. When the liquid and vapor boundaries are assessed at the same location ($Z_{L_b} = Z_{V_b}$), the value of α_e collapses to unity. As the vapor boundary is shifted right away from the defined liquid boundary location, it attains a minimum approximately half-way the decreasing density profile and increases until the end of the interphase region where a local maximum is attained. Shifting the liquid boundary to the right increases the local maxima and its location moves slightly to the left. Moving the liquid boundary towards the vapor phase implies that more molecules are considered to be in the liquid phase ($z < Z_{L_b}$). Hence, the mass flux of evaporating molecules increases which reflects back into an increase of the calculated evaporation coefficient.

Because of this sensitivity and the spread of the coefficients found in the literature [1, 10, 7], which were performed under the same thermodynamic conditions (temperature, pressure, density), an unique evaporation coefficient for each temperature cannot be defined. Since it is unclear where the exact location of the liquid and vapor boundary is and thus the value of the coefficient, we investigated the behaviour of coefficients for each temperature when different methods (Meland, Gu, Wolf) are combined. This implies that for the liquid boundary position, the method of Meland [7] or Gu [1] can be used. For the vapor boundary position, either the method of Meland, Gu or Wolf (alternative method) can be applied. Hence, 6 different combinations can be formed to determine the evaporation coefficient.

Our aim is to determine the range these coefficients can vary for a certain temperature T when different assumptions on the boundary positions are considered.

The results are depicted in Fig. 4 for different reduced temperatures. $L_B : X$ means that method X (Meland or Gu) is used to defined the liquid boundary position and $V_b : X$ means that method X (Meland, Gu or Wolf) is used for the vapor boundary position. This results in 6 different coefficients for each temperature for which an average value $\overline{\alpha_e}$ is calculated. These average values are used to fit a polynomial function (solid line), the standard deviation ($\pm 1\sigma$) are shown by the error overlines. The relative standard deviation (RSD), defined as $RSD = (\sigma/\overline{\alpha_e}) \times 100$, varies between 7%-10%.

As mentioned before, in case of an equilibrium state, the outgoing molecular velocity distribution

is assumed to be described by a half-range Maxwellian. Hence, the outgoing mass flux can be defined as $\langle J_{out} \rangle_e$, see Eq. (2). The influence of using Eq. (2) for the outgoing mass flux instead of the mass flux calculated from MD simulations, $\langle J_{out} \rangle_{MD}$, is depicted in Fig. 5. This has been done for all the 6 combinations of methods. A polynomial fit to the average values and $\pm 1\sigma$ bounds are also included. It can be observed that at low reduced temperatures (T/T_C), some of these methods predict the evaporation coefficient larger than unity. This is not possible according Eq. (1) because $\langle J_{ref} \rangle \geq 0$ which implies $\alpha_e \leq 1$.

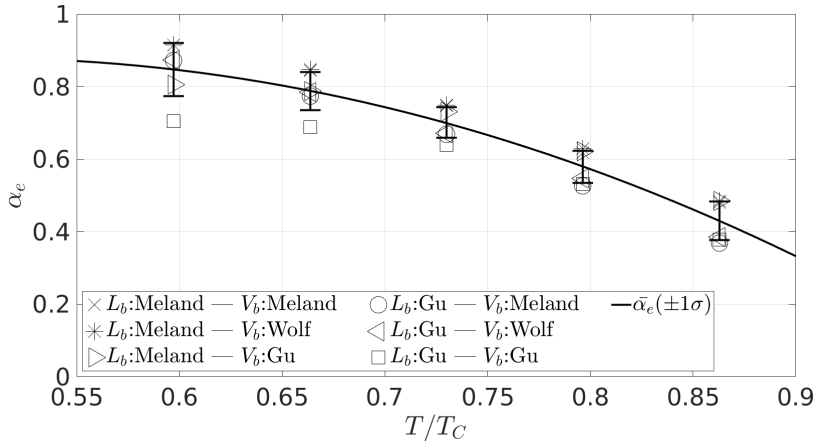

Figure 4: Evaporation/condensation coefficient as function of reduced temperature ($T_C = 150.7K$) for equilibrium MD simulations of Argon. $\langle J_{out} \rangle$ defined in Eq. (2) is calculated from MD simulation data.

When the vapor boundary location is determined with the method of Gu, the coefficient is much larger than unity for $T/T_C = 0.6\,(\alpha_e \approx 3)$ and $T/T_C = 0.66\,(\alpha_e \approx 1.5)$, both values are not shown in the Fig. 5. These values are related to the position of the vapor boundary which for low reduced temperatures $T/T_C \leq 0.73$ are predicted to be closer to the liquid phase for the method of Gu compared to Meland and Wolf. Therefore, it is reasonable to believe that the position of the vapor boundary is closer to the liquid phase compared to the position at which $\langle J_{out} \rangle_e = \langle J_{out} \rangle_{MD}$. Hence, $\langle J_{evap} \rangle_{MD}$ will not only capture evaporating molecules but also molecules reflecting back into the liquid phase so that $\langle J_{evap} \rangle_{MD} > \langle J_{out} \rangle_e$.

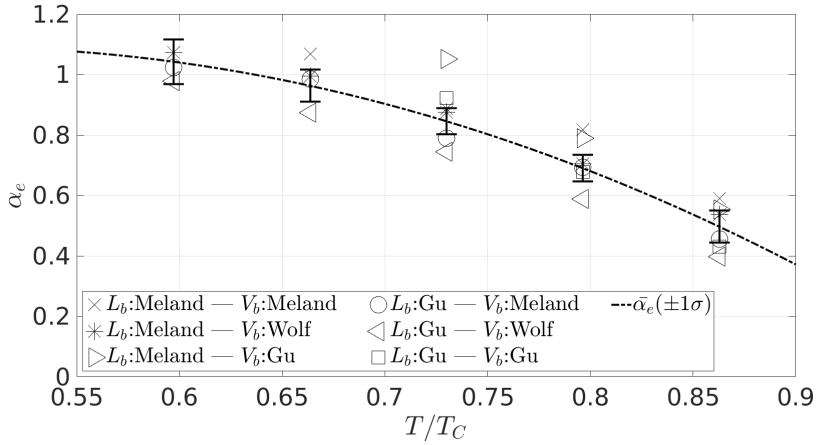

Figure 5: Evaporation/condensation coefficient as function of reduced temperature ($T_C = 150.7K$) for equilibrium MD simulations of Argon. $\langle J_{out} \rangle_{MD}$ defined in Eq. (1) is replaced by the equilibrium outgoing flux $\langle J_{out} \rangle_e$ defined in Eq. (2).

In Fig. 6 the previous obtained polynomial fits of the averaged evaporation coefficients (Fig. 4, Fig. 5) are plotted together with values from the literature. The results of Nagayama [13] are based on the transient state theory and are close to the average which also holds for the coefficients given by Ishiyama [2]. The values of Gu [1] are below the average and outside the $\pm 1\sigma$ bounds for all temperatures. This can be again related to the vapor boundary position. Especially for the low temperatures, $Z_{V_b}(Gu) < Z_{V_b}(Meland) < Z_{V_b}(Wolf)$ holds, with Z_{V_b} the position of the vapor boundary. According to Fig. 2, this implies that the coefficients of Gu will provide the lowest values in most cases.

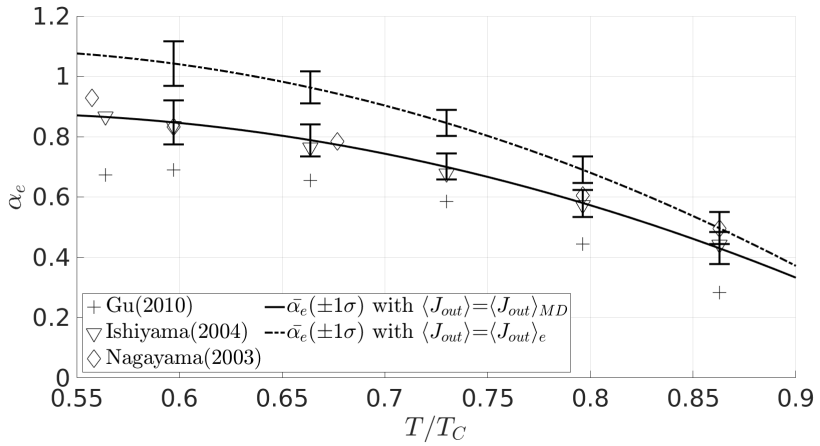

Figure 6: Evaporation/condensation coefficient as function of reduced temperature ($T_C = 150.7K$) for equilibrium MD simulations of Argon. The polynomial fits of the average coefficient $\overline{\alpha_e}$ and its $\pm 1\sigma$ shown in Fig.4 and Fig.5 are plotted with data from Gu [1], Ishiyama [2] and Nagayama [13].

5. Conclusions

- By shifting the vapor boundary from the liquid boundary towards the vapor phase, the behavior of the evaporation coefficient is explored in the interphase region. This lead to the development of an alternative method (Wolf) to determine the evaporation coefficient. Its local maximum attained in the interphase region, Fig. 2, is defined as the evaporation coefficient.

- Performing additional MD simulations like Gu and Ishiyama are unnecessary in the present simulation approach (Wolf). However, depending on which method is used for the liquid boundary, extra simulations may be required.

- Due to the influence of both boundaries on the evaporation coefficient and the spreading shown in the literature, a unique coefficient cannot be defined. We attributed to this by exploring the behavior of the evaporation coefficient when combining different methods to determine the liquid and vapor boundary positions. This lead to the introduction of an average evaporation coefficient $0.9 > \overline{\alpha_e} > 0.4$ as function of temperature with the relative standard deviation $RSD = \sigma/\overline{\alpha_e} \times 100$ varies between 7%-10%.

- Depending on which definition is used for the outgoing mass flux, $\langle J_{out}\rangle_{MD}$ or $\langle J_{out}\rangle_e$ (Eq. (2)), different average evaporation coefficients are obtained, Fig. 4 and Fig. 5. Coefficients larger than unity, shown in Fig. 5, are not possible. They are related to the position of the vapor boundary which will be located closer to the liquid phase compared to the position at which $\langle J_{out}\rangle_e = \langle J_{out}\rangle_{MD}$. Hence, $\langle J_{evap}\rangle_{MD}$ becomes larger than $\langle J_{out}\rangle_e$.

- The results of Ishiyama [2] and Nagayama [13] are close to the average value and within the $\pm 1\sigma$ bound, see Fig. 6. The results of Gu [1] are below the average and outside the $\pm 1\sigma$ bound.

Acknowledgements

This project has received funding from the European Union's Horizon 2020 research and innovation programme under the Marie Skłodowska-Curie grant agreement No. 643095.

References

[1] K. Gu, C.B. Watkins, and J. Koplik. Molecular dynamics simulation of the inverted temperature gradient phenomenon. *Fluid Phase Equilibria*, pages 77–89, 2010.

[2] T. Ishiyama, T. Yano, and S. Fujikawa. Molecular dynamics study of kinetic boundary condition at an interface between argon vapor and its condensed phase. *Physics of Fluids*, 16:2899, 2004.

[3] A.H. Persad and C.A.Ward. Expressions for the evaporation and condensation coefficients in the hertz-knudsen relation. *Chemical Reviews*, 116:7727–7767, 2016.

[4] T. Tsuruta, H. Tanaka, and T. Masuoka. Condensation/evaporation coefficient and velocity distributions at liquid–vapor interface. *Int. J. Heat and Mass Transfer*, 42:4107–4116, 1999.

[5] D.F. Hanks. *Evaporation from Nanoporous Membrane for High Heat Flux Thermal Management.* PhD thesis, MIT, 2016.

[6] I.A. Graur and A. Polikarpov. Comparison of different kinetic models for the heat transfer problem. *Int. J. Heat and Mass Transfer*, 46:237–444, 2009.

[7] R. Meland, A. Frezzotti, T. Ytrehus, and B. Hafskjold. Nonequilibrium molecular-dynamics simulation of net evaporation and net condensation, and evaluation of the gas-kinetic boundary condition at the interphase. *Physics of Fluids*, 16:223, 2004.

[8] M.C.W. Wolf, A. Polikarpov, A.J.H. Frijns, I. Graur, S.V. Nedea, , and R. Enright. Comparison of numerical results of molecular dynamics simulations and s-model kinetic equations for evaporation and condensation of argon. In *Proceedings of the 3rd European Conference on Non-equilibrium Gas Flows*, pages 275–278, 2018.

[9] M.C.W. Wolf, R. Enright, A.J.H. Frijns, S.V. Nedea, I. Graur, and A. Polikarpov. The position of the liquid and vapor boundaries and its influence on the evaporation/condensation coefficients. In *Proceedings of the 3rd MIGRATE International Workshop*, pages 56–59, 2018.

[10] K. Kobayashi, K. Hori, M. Kon, K. Sasaki, and M. Watanabe. Molecular dynamics study on evaporation and reflection of monatomic molecules to construct kinetic boundary condition in vapor–liquid equilibria. *J. Heat and Mass Transfer*, 52(9):1851, 2015.

[11] S. Plimpton. Fast parallel algorithms for short-range molecular dynamics. *J. Comp. Phys.*, 117:1–19, 1995.

[12] E.W. Lemmon, M.L. Huber, and M.O. McLinden. Reference fluid thermodynamic and transport properties-refprop. nist standard reference database 23,version 8.0. National Institute of Standards and Technology, 2007.

[13] G. Nagayama and T. Tsuruta. A general expression for the condensation coefficient based on transition state theory and molecular dynamics simulation. *J. Chemical Physics*, 118:1392, 2003.